PAPER • OPEN ACCESS
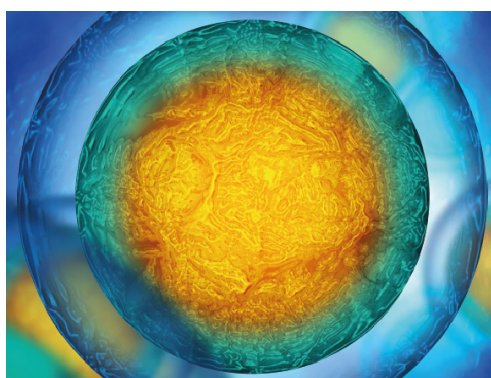
Fluid dynamics, scaling laws and plesiosaur locomotion

To cite this article: Ali Pourfarzan *et al* 2022 *Bioinspir. Biomim.* **17** 056007

View the article online for updates and enhancements.

Bioinspiration & Biomimetics

PAPER

Fluid dynamics, scaling laws and plesiosaur locomotion

Ali Pourfarzan[1], Donald M Henderson[2] and Jaime G Wong[1],*

[1] Department of Mechanical Engineering, University of Alberta, Edmonton, Canada
[2] Royal Tyrrell Museum of Palaeontology, Drumheller, Canada
* Author to whom any correspondence should be addressed.

E-mail: jgwong@ualberta.ca

Abstract

The evolutionary success of plesiosaurs has led to much attention regarding the dynamics of their locomotion. They exhibit identical tandem flippers, which is unique among all living and extinct species. However, these tandem flippers have been a source of debate regarding plesiosaurs' locomotion and behavior. Here we propose a new approach to studying plesiosaur locomotion based on universal scaling laws in fluid dynamics, which were used to estimate reduced frequency to characterize unsteadiness of an airfoil. It was found that, while the reduced frequency of plesiosaurs with high-aspect ratio flippers is similar to that of sea turtles, the most commonly used living analog, lower aspect ratio plesiosaurs were more similar in reduced frequency to penguins. This implies that plesiosaurs may have had large variations in agility among themselves, depending in particular on the specimen's flipper aspect ratio. While our results are consistent with the previous literature indicating a relationship between plesiosaur neck length and agility, our work supports broad and diverse analogies to living animals. Moreover, based on our results, cruising reduced frequency has some predictive value into manoeuvring behavior, rather than simply cruising behavior.

1. Introduction

The unique characteristic of plesiosaurs' tandem flippers, which is often referred to as the four-wing problem [1–3], has been a source of debate on their locomotion and, therefore, their behavior [1, 2, 4]. Apart from the study of how each of the individual flippers had moved, where the general consensus is on combination of antero-posterior and dorso-ventral motion [2], contradicting hypotheses have been suggested to explain the biomechanics of why plesiosaurs had two sets of wing-like flippers while all living marine tetrapods have only one [2, 5]. Some silhouettes of plesiosaurs with varied body planforms can be found in figure 5, in later sections, as a reference for readers unfamiliar with these animals. Due to the close resemblance of plesiosaur flippers to other hydrodynamic planforms such as engineered hydrofoils, one approach to the four-wing problem has come from engineering perspective [2], where the assumption that the animal sought to maximize efficiency and thrust coefficients in cruising conditions

was used to elucidate how the flow from both sets of flippers interacted in propulsion.

Flapping wings and flippers produce a trailing vortex wake [6]. It has been shown that there is an upper limit for the quantity of mass that can be fed into a vortex before secondary vortices form [7, 8], known as optimal vortex formation. Those vortices formed on a wing are no different, with optimal vortex formation being described in this case with the Strouhal number [8]. The Strouhal number of an oscillating wing is defined as:

$$St = \frac{fA}{U_\infty}, \qquad (1)$$

where f is the frequency of oscillation, A is peak-to-peak amplitude of the oscillation of the wing or flipper, and U_∞ is the forward velocity. In cruising conditions, the Strouhal number of flapping propulsion—in both air and water, from length-scales ranging from insects to whales—is observed in a limited range of $0.2 < St < 0.4$ [9, 10]. It must be emphasized that this limited range occurs over a

wide range of length and velocity scales, occurring identically over a wide range of flow regimes. The Strouhal number is typically described as measurement of flapping amplitude, closely associated with force generation [11]. Reduced frequency, meanwhile, is a closely-related dimensionless number describing the unsteadiness of a flapping motion [12]:

$$k = \frac{\pi f c}{U_\infty},\qquad(2)$$

where f is the flapping frequency, and c is chord of the wing or flipper. Reduced frequency is a ratio of time scales between the flow and the oscillatory wing motion. The reduced frequency can also be used to describe the time-scale on which aerodynamic or hydrodynamic forces can change. For instance, in a study of atmospheric gusts by Wong *et al* [13], the characteristic time scale (T) of a passing gust was defined based on the time between the maximum and minimum effective angle of attack imposed on an aerodynamic surface, which was used to relate the flow velocity to the gust wavelength, $\lambda = U_\infty T = \frac{U_\infty}{f}$. This can be expressed equivalently in terms of the reduced frequency:

$$k = \frac{\pi c}{\lambda},\qquad(3)$$

where the reduced frequency here takes the form of a ratio between the length-scales of the aerodynamic surface, c, and of the gust wavelength, λ. A smaller gust wavelength (λ) represents a more rapid change of ambient conditions. This in turn means smaller time scale (T), and smaller time scale represents how quickly force can change with respect to the flow velocity or forward speed. When studying the flow field of simplified goose-like flight, Hubel and Tropea found that the effect of unsteady flow phenomena is considerable on vortex shedding and force coefficients even at low reduced frequencies [14]. Generally, studies have shown that, while thrust increases with reduced frequency, high efficiencies are achieved at relatively low reduced frequencies [15]. Analogous results have been found for Strouhal number in swimming animals. For example, Borazjani and Daghooghi observing greater force amplitudes at higher Strouhal numbers, and greater efficiency at lower values [16]. Likewise, Borazjani and Daghooghi noted that vortex shedding was more likely at higher Strouhal numbers.

In this article, we propose an alternative approach to study the flippers of extinct animals such as plesiosaurs, in the context of universal scaling rules in fluid dynamics, such as the convergence of Strouhal number for all flapping animals on values in the range $0.2 < St < 0.4$ for cruising conditions [9, 10]. Using the established convergence in Strouhal number, we derive a geometric relationship between it and the reduced frequency. This particular geometric scaling embeds properties, such as the aspect ratio, known to relate to agility [17]. Reduced frequency does not

exhibit the universal convergence in the way Strouhal number does. However, due to this embedding of properties, such as the aspect ratio, the cruising reduced frequency can correlate to agility even in non-cruising conditions. For example, dragonflies, known for their high maneuverability, have relatively high reduced frequencies, while sea turtles have lower reduced frequencies associated with limited maneuverability, even though they both cruise at similar Strouhal numbers. The quality of this correlation is low, and may lose its meaning altogether when comparing across different propulsion modes, such as comparing the flapping of tail-fins to flapping wing-like flippers. However, in the context of plesiosaur locomotion, where no direct measurements of turn rates or accelerations are possible, this may provide an additional point of reference in determining their relative manoeuvring performance, and therefore in reconstructing their ecological role and behavior. Moreover, it is common to use the behavior of living animals to estimate the behavior of extinct ones. We believe that the ability to evaluate the reduced frequency of extinct animals provides additional context in evaluating model organisms in this way. Therefore, our study introduces a new perspective to study plesiosaur locomotion by comparing its unsteadiness to that of existing animals. This proposed methodology of investigating plesiosaur agility is consistent with prior findings in literature that plesiosaurs with low aspect ratio flippers are more likely to have had relatively higher unsteadiness and agility levels, while high aspect ratio plesiosaurs are likely to have exhibited lower agility [18]. However, rather than a simple relative scale among plesiosaurs in isolation, as was already possible with aspect ratio information alone [18], characterizing unsteadiness in terms of the reduced frequency permits us to more readily compare plesiosaurs to living taxa. Our methodology is also consistent with literature citing neck-length as a limiting factor in maneuverability [19, 20], as neck length further correlates with reduced frequency as presented here.

2. Materials and methods

In this study, to predict plesiosaur's agility level, we follow a multistage approach. First, we propose and validate a model to predict the reduced frequency of variety of flapping appendages using only their physical layout, similar to the information that would be available from fossil data. Following this validation, we predict a sea turtle's reduced frequency only using the data obtained from its skeleton and compare it to the actual reduced frequency calculated using the kinematics of a living sea turtle as second validation. Finally, we apply this model to plesiosaur fossils with different flipper sizes and body planforms to predict their agility level.

2.1. A mathematical model to predict behavior

As mentioned in the previous sections, reduced frequency will be used as a metric for agility in this study, with the caveats mentioned above. Although reduced frequency does not converge to a specific range of values as Strouhal number does, some aspects of the animal behaviour can be inferred from its value. For example, insects typically have higher reduced frequencies than seabirds, and in turn, are also associated with greater agility. However, reduced frequency is usually observed directly. Therefore, to predict the reduced frequency of an extinct species where swimming speed and flapping frequency are unknown, we must eliminate the ratio f/U from the expression in equation (2). As this ratio also appears in Strouhal number, we can replace the ratio with a function of Strouhal number:

$$k = St \frac{\pi c}{\theta_0 b},\tag{4}$$

where θ_0 (rad) is stroke angle (dorso-ventral), and b is span of the wing. The product of stroke angle and span is used as an estimate of flapping amplitude as the stroke angle, span and chord of plesiosaurs can be estimated from fossil remains. Together with the observation that the Strouhal number is approximately a constant for flapping locomotion, this reduces the cruising reduced frequency to a geometric property of the flipper and its joints. The specific value $St = 0.35$ is used in this study as a characteristic value, coinciding with maximum thrust coefficient and within the range of observed values in nature [9]. It is worth noting, however, that small variations from this value do not appreciably alter the conclusions in later sections.

2.2. Kinematic data

Kinematic data of 47 existing flying and swimming animals including eight birds [21–26], 12 bats [27], 10 insects [28–31], three reptiles [32, 33], four aquatic birds [34, 35], nine marine mammals [36–38] and one fish [39] ($n = 62$ cases) have been collected from the open literature to calculate the Strouhal number and actual reduced frequency of each animal, as well as the predicted reduced frequency using equations (1), (2) and (4), respectively (see supplementary material (https://stacks.iop.org/BB/17/056007/mmedia) data S1). The kinematic data used to calculate the actual and predicted reduced frequencies have been acquired from the same source for each specimen. If a range of values rather than an exact value was given for a specific parameter such as cruising speed, the average value of the provided range is used for the calculations. Where flipper chord was not measured, we calculated the chord as $c = \frac{S}{b} = \frac{b}{AR}$, where c is the chord, S is the flipper area, b is the flipper span (measured from the flipper root to the flipper tip), and AR is the aspect ratio of the flipper. If flapping amplitude was provided
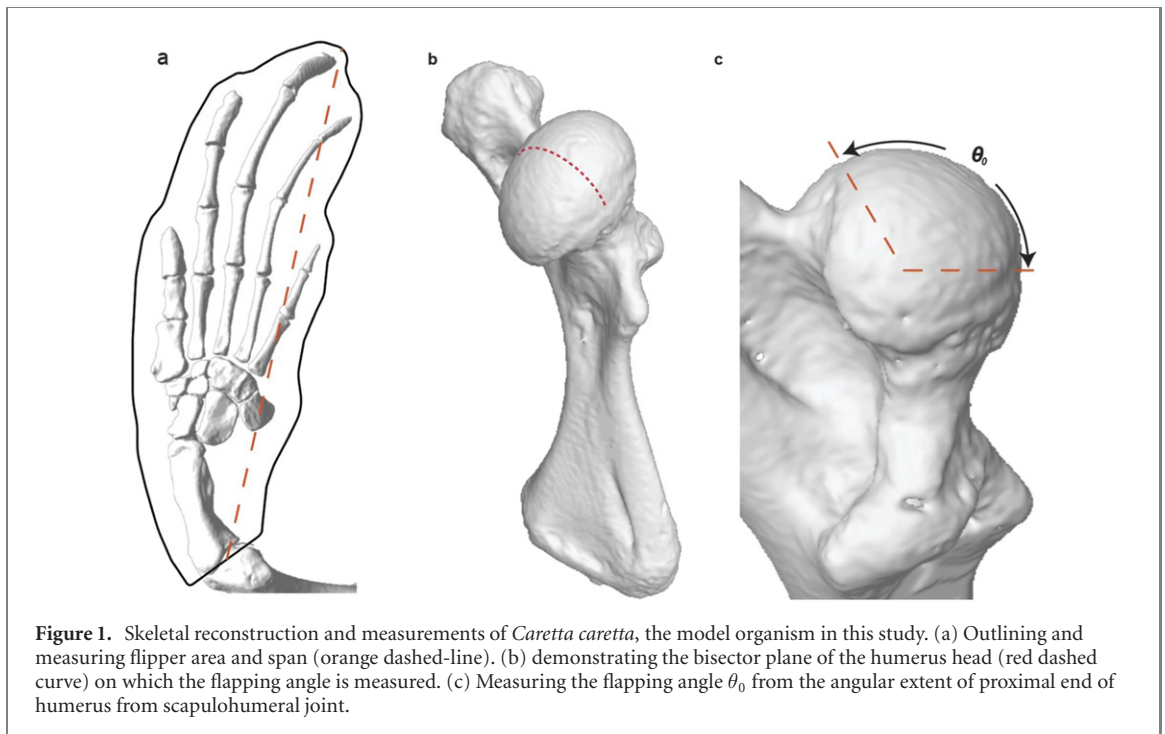
instead of flapping angle, we approximated the angle as $\theta_0 = 2\sin^{-1}(\frac{A}{2b})$, where θ_0 is flapping angle, A is peak-to-peak flapping amplitude and b is flipper span. If data for a parameter in equations (1), (2) and (4) was not reported for a specific animal in the reference literature, an additional source such as a different literature or online videos have been used to estimate an approximate value for the missing measurement, which is provided in the supplementary material data S1 as additional source. For living sea turtles, an average value for the flapping frequency and the flapping angle is used to estimate reduced frequencies. As data for these parameters were missing in the reported literature, we measured them from online videos, which the source link and measuring time is provided in the supplementary material data S2 as reference.

2.3. Sea turtle skeletal measurements

To measure the flapping angle from sea turtle skeletons, computed tomography (CT) scans of the humerus of a *Caretta caretta*, a *Chelonia mydas* and an *Eretmochelys imbricata* were gathered from an online resource. The CT scans are provided via Harvard Museum of Comparative Zoology (see supplementary material data S3 for citation and specimen numbers). A complete flipper CT scan of an adult *Caretta caretta* was gathered from Royal Veterinary College to measure both flapping angle and flipper aspect ratio (see supplementary material data S3 for the reference). A three-dimensional (3D) skeletal model is reconstructed via Object Research Systems Dragonfly software. Skeletal measurements have been done via ImageJ software. To estimate the flipper aspect ratio as $AR = \frac{b^2}{S}$, the flipper area was outlined and measured as seen in figure 1(a). The flipper span was measured from the joint between humerus and ulna and radius to the tip of the phalanges. The head of the humerus is analogous to a 3D, tri-axial ellipsoid, where the flapping angle takes place about the longest axis of this ellipsoid. Flapping angles were measured from the angular extent of proximal end of humerus from scapulohumeral joint and about the longest axis (figures 1(b) and (c)). The plane on which flapping angle was measured is the bisector of the humerus head and the center of the rotation is the center of the angular extent of the proximal end of humerus. The measurements are presented in the supplementary material data S3.

To provide an estimate of the limit that articular cartilage in the scapulohumeral joint, along with the muscle traction, can exert on the limb movement in the dorso-ventral direction, we can subtract the average flapping angles of swimming sea turtles measured from online videos (122.13 degrees) from the average flapping angle measured directly from skeletons (136.37 degrees). This provides cartilage limits of approximately 14.56 degrees in the dorso-ventral direction. Based on our measurement process, further

Figure 1. Skeletal reconstruction and measurements of *Caretta caretta*, the model organism in this study. (a) Outlining and measuring flipper area and span (orange dashed-line). (b) demonstrating the bisector plane of the humerus head (red dashed curve) on which the flapping angle is measured. (c) Measuring the flapping angle θ_0 from the angular extent of proximal end of humerus from scapulohumeral joint.

discussion will only take the first two significant digits (15 degrees) when accounting for cartilage limits.

2.4. Plesiosaur skeletal measurements

To predict the reduced frequency of plesiosaurs using equation (4) using kinematic data, we performed complete measurements of the aspect ratio and flapping angle of three individual plesiosaurs: *Trinacomerum osbornii*, *Albertonectes vanderveldei*, and 'Parson's Creek'. For the specimens such as *Thalassomedon hanningtoni*, *Cryptoclidus oxoniensis*, 'Sage Creek', *Liopleurodon ferox*, *Nicholls saura borealis*, *Rhomaleosaurus thorntoni*, *Tatenectes laramiensis*, *Brancasaurus* and *Meyerosaurus* that we were unable to measure the flapping angle due to the fossil conditions, we only measured their aspect ratio. For the flapping angle of these specimens, we used an average value and a range of measured flapping angles of other specimens in the Royal Tyrell Museum to address the uncertainty range of their reduced frequency. The effect and limitations of applying this approximation is discussed in the next section. To estimate the flipper aspect ratio as $AR = \frac{b^2}{S}$, the flipper area has been measured in the same way as sea turtles using an internally developed script which is explained in details in reference [40]. Figure 2 demonstrates the fore flipper and humerus of *Trinacomerum osbornii*. The span is determined by finding the maximum perimeter distance from the midpoint of base of the flipper (figure 2(a)). Flapping angles were measured from the proximal end of humerus and femur (figure 2(a)). Figures S1 and S2 in the supplementary material demonstrate the annotated flipper images of *Albertonectes vanderveldei* and 'Parson's Creek', respectively.

From plesiosaur remains, like most flapping-like motion, both antero-posterior and dorso-ventral motions are possible for plesiosaur flippers. However, for most flapping wings and flippers observed in nature, dorso-ventral motion is the dominant motion responsible for propulsion. Therefore, we predicted reduced frequency of plesiosaur considering the dorso-ventral angle. In well preserved specimens of plesiosaurs the humeral head can be seen to be almost hemispherical. There is a distinct difference in bone texture between the surface of the head of the humerus and the lateral surface of the remainder of the bone. The head is either smooth, or distinctly pitted with a texture unlike that of lateral surface. The junction of these two surfaces was taken as defining the perimeter of the head. In many cases there is also a raised rim at the junction of the two surfaces (figure 2(b)). To estimate the angular extent of the humeral head two co-terminal radii were positioned so that they tangentially contacted opposite sides of the head, and had their common origin located within the bone, but at an arbitrary distance from the head. This distance was set by the configuration of the radii and their points of tangency to the head. This measuring was either done graphically with a digital photograph in the drawing program CorelDRAW or done with a large protractor and two rulers on physical specimens. The true size and extent of the original soft tissue comprising the cartilage covering of the head of the humeri of the extinct plesiosaurs is unknowable. It was decided to infer conservative estimates of the flapping angles such that they would stay within the observed angular extent of head of the humerus and the selected values are compatible with the observed angular extents of the smooth-headed
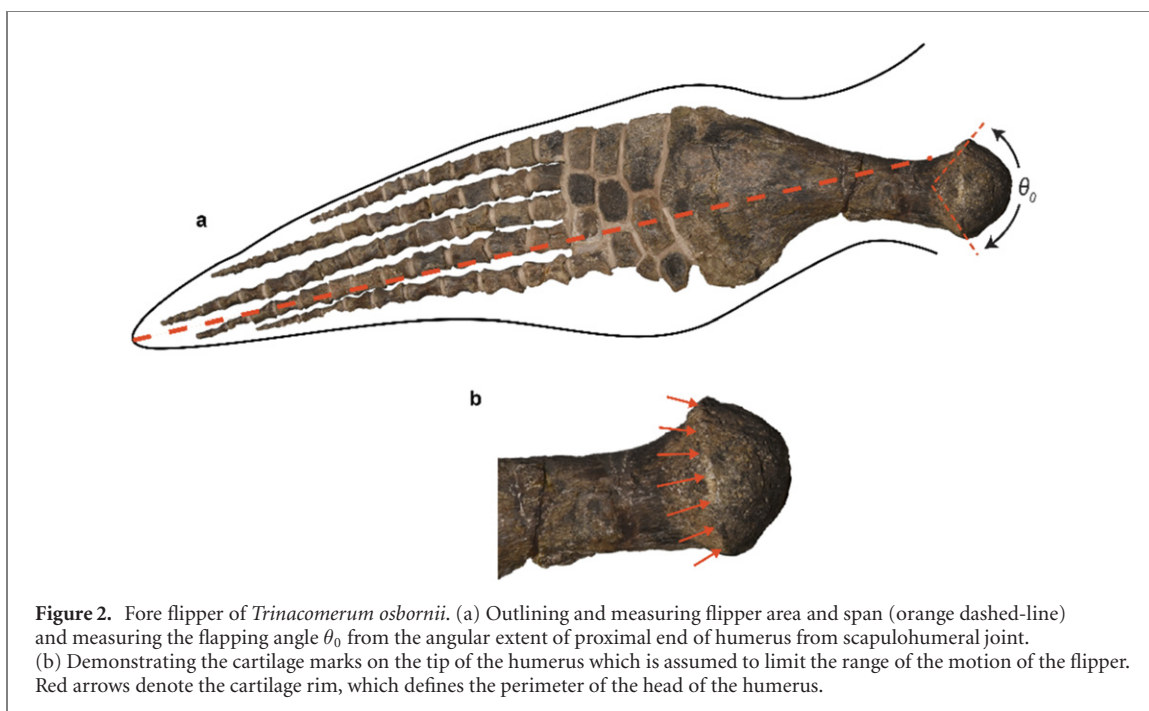
Figure 2. Fore flipper of *Trinacomerum osbornii*. (a) Outlining and measuring flipper area and span (orange dashed-line) and measuring the flapping angle θ_0 from the angular extent of proximal end of humerus from scapulohumeral joint. (b) Demonstrating the cartilage marks on the tip of the humerus which is assumed to limit the range of the motion of the flipper. Red arrows denote the cartilage rim, which defines the perimeter of the head of the humerus.

portions of the humeri (figure 2(b)). The measurements, specimen numbers and related references are presented in the supplementary material data S3 for each specimen.

3. Results and discussion

To validate the model for reduced frequency presented in equation (4), we calculated the actual reduced frequency of a wide range of 47 existing flying and swimming animals [21–39] ($n = 62$ cases) from data available in open literature, and compared these values to those predicted by equation (4). The comparison between actual reduced frequency and predicted reduced frequency has been made only for animals whose Strouhal number corresponded to cruising conditions [9, 10] ($0.2 < St < 0.4$). This comparison is presented in figure 3, and shows a good agreement between our model and observed values, within the 95% prediction interval. We followed the standard procedure for all statistical analysis including regression, two-sided prediction intervals and mean squared error [41] for our data collected from open literature in figure 3.

Flapping angles in figure 3 were determined from the behavior of living animals. In order to validate our model when data is limited to that obtained from fossil remains, a second validation was performed by applying the model to a living species, a sea turtle, using both skeletal data, and observed behavior. Sea turtles are chosen for this validation due to their common use as a model for plesiosaurs [4, 5]. Data such as flipper area, span and flapping angle are obtained from CT scans of an adult sea turtle, *Caretta carretta*, simulating skeletal remains (figure 1). Flapping angles were measured from the angular extent

of proximal end of humerus from scapulohumeral joint. To account for the reduction of mobility caused by cartilage or muscle traction on the dorso-ventral flapping angle, an average of observed flapping angles from living sea turtles was deducted from the average of the flapping angles measured from skeletons. The predicted reduced frequency from a sea turtle skeleton was found to be $k = 0.13$, which was slightly lower than the average value of reduced frequency observed in nature, $k = 0.14$, where the difference is approximately 7%. This comparison shows that our proposed model is able to predict an animal's reduced frequency, and thus estimate its relative agility, using only the data obtained from skeletal remains.

Following the aforementioned validation, we applied our model to plesiosaur fossils to predict each specimen's reduced frequency. The results are shown in figure 4. For the plesiosaurs from which we were unable to measure the flapping angle, we introduced an uncertainty range of reduced frequency as function of flapping angle, since flapping angle has a linear effect on reduced frequency as modelled here in equation (4). The results of this analysis are included in figure 4, where the squares denote the average value of the flapping angles measured from fossil remains of well-preserved specimens, i.e. *Trinacomerum osbornii*, *Albertonectes vanderveldei*, and 'Parson's Creek' plesiosaurs. Calculated values of reduced frequency for each of the specimens is presented in the supplementary material table S1. The uncertainty range of reduced frequency for the measured range of flapping angles was found to be sufficiently small to have no effect on our conclusions. Rather, we observe here greater variations among plesiosaurs with respect to aspect ratio than from uncertainty or variation in flapping angle. This observation was limited by the
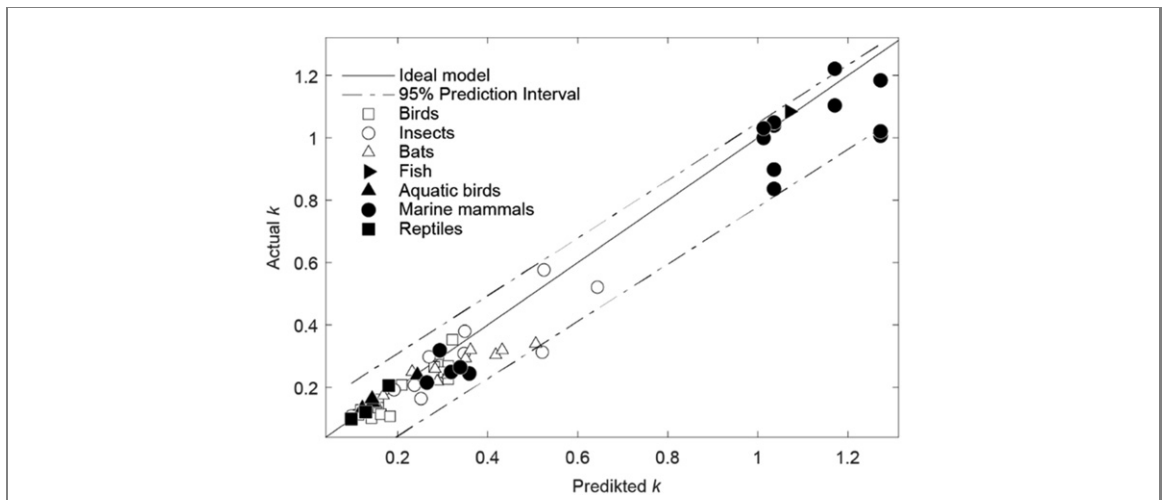
Figure 3. A comparison of predicted reduced frequency with and actual reduced frequency. The comparison has been made for 47 flapping species ($n = 62$) in cruising condition within the range of $0.2 < St < 0.4$. The regression coefficient of our model is 0.92, the determination coefficient is 0.96 and the mean squared error is estimated as 0.004. The ideal model is illustrated as a continuous black line with slope of 1. It can be seen that the proposed model can predict reduced frequency accurately, as data are clustered around the ideal model.
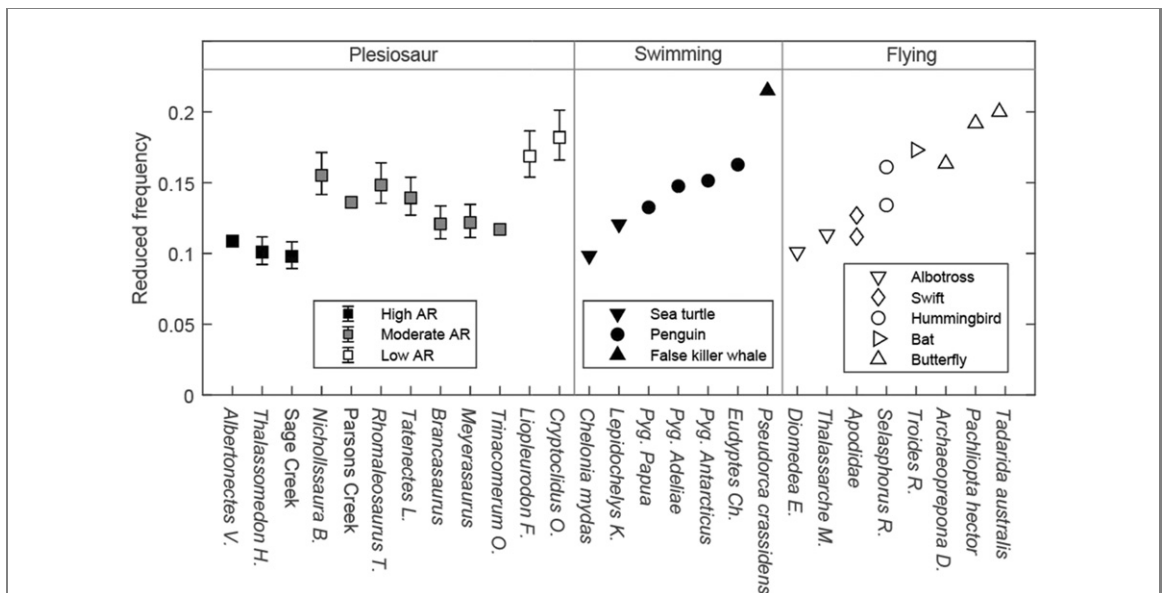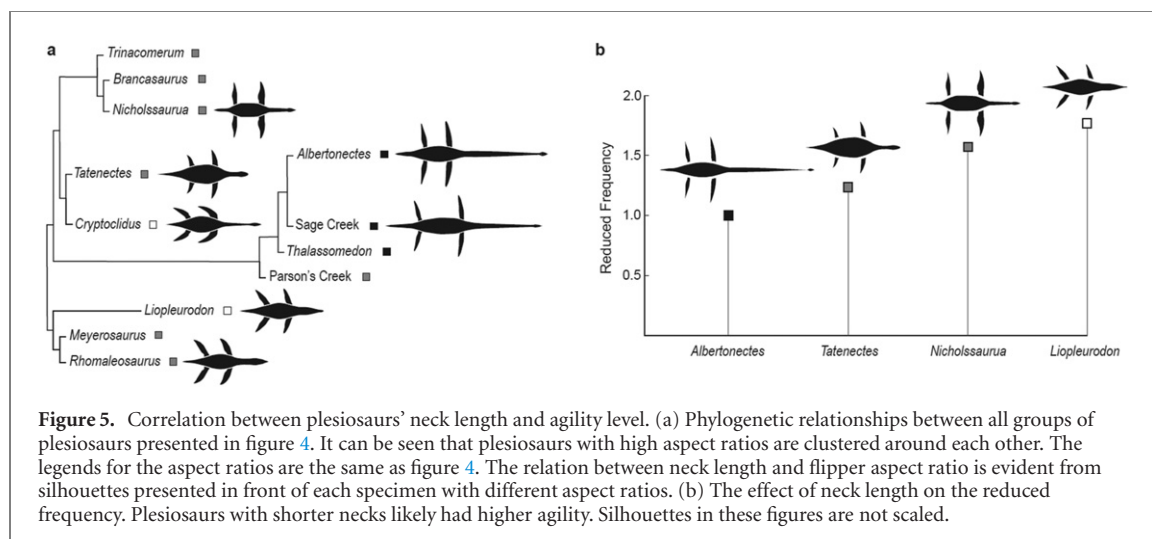

Figure 4. Reduced frequency of existing swimming and flying animals matching the reduced frequency of plesiosaurs. The square markers on each of the uncertainty bars, seen for the plesiosaur data, represent the reduced frequency estimate derived from the average flapping angle of well-preserved specimens. This process was repeated for each group of low, moderate and high aspect ratio flippers. Plesiosaur specimens might have had different level of agility among themselves depending on the flipper aspect ratio. Sea turtles are appropriate model organism only for specific subset of plesiosaurs.

number of independent flapping angle estimations that could be obtained, and so should not be considered an independent conclusion. However, this observation was used to conceptually group different plesiosaur specimens.

The role of aspect ratio is demonstrated when we compare the span length of *Cryptoclidus oxoniensis*, with lowest aspect ratio ($AR = 3.45$) among all plesiosaurs, and *Tatenectes laramiensis* which has moderate aspect ratio flippers ($AR = 4.90$). Although they have similar span lengths, their predicted reduced frequency in figure 4 reveals that *Cryptolidus*

oxoniensis likely had greater agility. Therefore, we grouped plesiosaurs into three groups based on high ($AR > 6$), moderate ($4 < AR < 6$), and low ($AR < 4$) flipper aspect ratios, which correspond to low, moderate, and high reduced frequencies. Living species with similar reduced frequencies to that predicted for plesiosaurs are presented in figure 4. This figure also shows that the reduced frequency in cruising conditions gives approximation of agility among living species, based on what we can observe from the behavior of animals in nature. This provides evidence that the reduced frequency in cruising conditions

Figure 5. Correlation between plesiosaurs' neck length and agility level. (a) Phylogenetic relationships between all groups of plesiosaurs presented in figure 4. It can be seen that plesiosaurs with high aspect ratios are clustered around each other. The legends for the aspect ratios are the same as figure 4. The relation between neck length and flipper aspect ratio is evident from silhouettes presented in front of each specimen with different aspect ratios. (b) The effect of neck length on the reduced frequency. Plesiosaurs with shorter necks likely had higher agility. Silhouettes in these figures are not scaled.

offers some predictive power regarding the agility of the animal. As seen in figure 4, the *Albertonectes vanderveldei*, 'Sage Creek' and *Thalassomedon* specimens have relatively low reduced frequencies, similar to sea turtles and albatrosses. Meanwhile, *Cryptoclidus oxoniensis* with the lowest aspect ratio has the highest reduced frequency, similar to that of penguins and hummingbirds, each known for their ability to rapidly change direction. Therefore, we conclude that plesiosaurs likely had significant variation among themselves in terms of agility and acceleration. Morphometric phylogenetic analysis conducted in previous studies also reported the possible variation in swimming techniques between different clades based on differences in girdle and limb morphology among plesiosaurs [4, 42]. Furthermore, this finding suggests that sea turtles are unlikely to be an appropriate model organism for all plesiosaurs, and rather they are a good analog for the subset of these prehistoric marine reptiles with larger aspect ratios. Figure S3 in the supplementary material shows direct comparisons between aspect ratio, flapping angle, and reduced frequency for the specimens in figure 4 for additional clarity of the above observations.

Finally, we have observed that long-necked plesiosaurs consistently have high-aspect ratio flippers. In the literature, the length of the neck is understood to have an influence on maneuverability [19, 20]. Plesiosaurs with longer necks are assumed to be ambush predators due to the limitations that such long necks would likely have on their ability to turn, whereas species with short or moderate necks are more likely active predators [1, 19, 20, 43, 44]. Our findings are consistent with this hypothesis. Silhouettes of some of the specimens in figure 4 are presented in figure 5 to illustrate this observation. The phylogenetic tree for the plesiosaur specimens considered in this study [45], as shown in figure 5, shows that the correspondence between swimming behavior and lineage is most pronounced for the long-necked specimens. Although high aspect ratio

plesiosaurs with low reduced frequencies are clustered around each other, low and moderate aspect ratio specimens are spread out in the cladogram, suggesting that, whereas the long neck is a significant constraint on effective propulsive behavior, a broader set of strategies are possible for the plesiosaur's four flipper layout generally.

4. Conclusion

A new method was introduced to study the locomotion of extinct animals such as plesiosaurs using a universal scaling rule found in animal locomotion. In this study, reduced frequency, which determines the unsteadiness of a flapping motion, was considered as the similarity parameter to compare the swimming behavior of plesiosaurs to living taxa. A geometric relationship was derived between the Strouhal number and the reduced frequency, based on the established convergence on a small range of Strouhal numbers for cruising conditions in nature, which correspond to maximum efficiency. Following this derivation, the geometric relationship derived for cruising conditions, embedded flipper aspect ratio, a parameter which correlates to agility and is used previously to rank plesiosaurs based on maneuverability in non-cruising conditions [18]. Direct observations of manoeuvrability, such as observing velocity and acceleration in swimming and flight, is obviously impossible for extinct species. Therefore, given the limited tools available for paleontologists and other researchers, we hope the methodology proposed here will be a useful supplement to existing techniques for estimating swimming or flying behavior.

The proposed model for reduced frequency allowed us to accurately predict the reduced frequencies of living animals using geometric data such as flipper aspect ratio and the flapping angle, with the Strouhal number as the only kinematic parameter, which was chosen based on the universal convergence, i.e., $St = 0.35$. Applying the model to sea turtles

using data obtained from structural, skeletal information, the predicted reduced frequency compared favorably to the reduced frequency observed in nature with approximately 7% difference, which validated the extension of our method to the cases in which data is limited to structural information, such as that obtained from fossils.

Following a comparison between the reduced frequency of plesiosaurs and living animals, we concluded that plesiosaurs likely had a wide range of agility levels among themselves. For example, while the reduced frequency of high aspect ratio plesiosaurs matched closely to sea turtles, the reduced frequency of low aspect ratio plesiosaurs was likely closer to that of penguins, well known for their underwater agility and speed. This is consistent with the findings of previous studies that have considered the constraint of neck length on plesiosaur agility [19, 20], as these animals all exhibit high aspect ratios, and therefore low reduced frequencies.

Acknowledgments

Data availability statement

All data that support the findings of this study are included within the article (and any supplementary files).

ORCID iDs

Jaime G Wong ⓘ https://orcid.org/0000-0002-0364-4405

Reference

[1] Halstead L B 1989 Plesiosaur locomotion *J. Geol. Soc.* **146** 37–40

[2] Muscutt L E, Dyke G, Weymouth G D, Naish D, Palmer C and Ganapathisubramani B 2017 The four-flipper swimming method of plesiosaurs enabled efficient and effective locomotion *Proc. R. Soc.* B **284** 20170951

[3] Lingham-Soliar T 2000 Plesiosaur locomotion is the four-wing problem real or merely an atheoretical exercise? *Neues Jahrbuch Geol. Palaontol. Abhand.* **217** 45–87

[4] Carpenter K, Sanders F, Reed B, Reed J and Larson P 2010 Plesiosaur swimming as interpreted from skeletal analysis and experimental results *Trans. Kans. Acad. Sci.* **113** 1–34

[5] Liu S, Smith A S, Gu Y, Tan J, Liu C K and Turk G 2015 Computer simulations imply forelimb-dominated underwater flight in plesiosaurs *PLoS Comput. Biol.* **11** e1004605

[6] Wong J G and Rival D E 2015 Determining the relative stability of leading-edge vortices on nominally two-dimensional flapping profiles *J. Fluid Mech.* **766** 611

[7] Gharib M, Rambod E and Shariff K 1998 A universal time scale for vortex ring formation *J. Fluid Mech.* **360** 121–40

[8] Dabiri J O 2009 Optimal vortex formation as a unifying principle in biological propulsion *Annu. Rev. Fluid Mech.* **41** 17–33

[9] Triantafyllou M S, Triantafyllou G S and Gopalkrishnan R 1991 Wake mechanics for thrust generation in oscillating foils *Phys. Fluids* A **3** 2835–7

[10] Taylor G K, Nudds R L and Thomas A L R 2003 Flying and swimming animals cruise at a Strouhal number tuned for high power efficiency *Nature* **425** 707–11

[11] Baik Y S, Bernal L P, Granlund K and Ol M V 2012 Unsteady force generation and vortex dynamics of pitching and plunging aerofoils *J. Fluid Mech.* **709** 37

[12] Birnbaum W 1924 Das ebene problem des schlagenden Flügels *Z. Angew. Math. Mech.* **4** 277–92

[13] Wong J G, Mohebbian A, Kriegseis J and Rival D E 2013 Rapid flow separation for transient inflow conditions versus accelerating bodies: an investigation into their equivalency *J. Fluids Struct.* **40** 257–68

[14] Hubel T Y and Tropea C 2010 The importance of leading edge vortices under simplified flapping flight conditions at the size scale of birds *J. Exp. Biol.* **213** 1930–9

[15] Wu X, Zhang X, Tian X, Li X and Lu W 2020 A review on fluid dynamics of flapping foils *Ocean Eng.* **195** 106712

[16] Borazjani I and Daghooghi M 2013 The fish tail motion forms an attached leading edge vortex *Proc. R. Soc.* B **280** 20122071

[17] Vogel S 1994 *Life in Moving Fluids* 2nd edn (Princeton, NJ: Princeton University Press)

[18] O'Keefe F R 2001 Ecomorphology of plesiosaur flipper geometry *J. Evol. Biol.* **14** 987–91

[19] Troelsen P V, Wilkinson D M, Seddighi M, Allanson D R and Falkingham P L 2019 Functional morphology and hydrodynamics of plesiosaur necks: does size matter? *J. Vertebr. Paleontol.* **39** e1594850

[20] Wintrich T, Jonas R, Wilke H-J, Schmitz L and Sander P M 2019 Neck mobility in the Jurassic plesiosaur cryptoclidus eurymerus: finite element analysis as a new approach to understanding the cervical skeleton in fossil vertebrates *PeerJ* **7** e7658

[21] Spedding G R 1987 The wake of a kestrel (Falco tinnunculus) in flapping flight *J. Exp. Biol.* **127** 59–78

[22] Pennycuick C 1996 Wingbeat frequency of birds in steady cruising flight: new data and improved predictions *J. Exp. Biol.* **199** 1613–8

[23] Tobalske B W, Warrick D R, Clark C J, Powers D R, Hedrick T L, Hyder G A and Biewener A A 2007 Three-dimensional kinematics of hummingbird flight *J. Exp. Biol.* **210** 2368–82

[24] Stalnov O, Ben-Gida H, Kirchhefer A J, Guglielmo C G, Kopp G A, Liberzon A and Gurka R 2015 On the estimation of time dependent lift of a European starling (Sturnus vulgaris) during flapping flight *PLoS One* **10** e0134582

[25] Rosén M, Spedding G R and Hedenström A 2004 The relationship between wingbeat kinematics and vortex wake of a thrush nightingale *J. Exp. Biol.* **207** 4255–68

[26] Henningsson P, Spedding G R and Hedenström A 2008 Vortex wake and flight kinematics of a swift in cruising flight in a wind tunnel *J. Exp. Biol.* **211** 717–30

[27] Bullen R D and McKenzie N L 2002 Scaling bat wingbeat frequency and amplitude *J. Exp. Biol.* **205** 2615–26

[28] Betts C R and Wootton R J 1988 Wing shape and flight behaviour in butterflies (Lepidoptera: Papilionoidea and Hesperioidea): a preliminary analysis *J. Exp. Biol.* **138** 271–88

[29] Rüppell G 1989 Kinematic analysis of symmetrical flight manoeuvres of Odonata *J. Exp. Biol.* **144** 13–42

[30] Dudley R 1990 Biomechanics of flight in neotropical butterflies: morphometrics and kinematics *J. Exp. Biol.* **150** 37–53

[31] Ennos A R 1989 The kinematics and aerodynamics of the free flight of some Diptera *J. Exp. Biol.* **142** 49–85

[32] Davenport J, Munks S A and Oxford P J 1984 A comparison of the swimming of marine and freshwater turtles *Proc. R. Soc.* B **220** 447–75

[33] LeBuff C R 1990 *The Loggerhead Turtle in the Eastern Gulf of Mexico, Caretta* (Sanibel: Research Inc.) p 216

[34] Wilson R and Liebsch N 2003 Up-beat motion in swinging limbs: new insights into assessing movement in free-living aquatic vertebrates *Mar. Biol.* **142** 537–47

[35] Sato K, Shiomi K, Watanabe Y, Watanuki Y, Takahashi A and Ponganis P J 2010 Scaling of swim speed and stroke frequency in geometrically similar penguins: they swim optimally to minimize cost of transport *Proc. R. Soc.* B **277** 707–14

[36] Fish F 1998 Comparative kinematics and hydrodynamics of odontocete cetaceans: morphological and ecological correlates with swimming performance *J. Exp. Biol.* **201** 2867–77

[37] Fish F E, Innes S and Ronald K 1988 Kinematics and estimated thrust production of swimming harp and ringed seals *J. Exp. Biol.* **137** 157–73

[38] Videler J and Kamermans P 1985 Differences between upstroke and downstroke in swimming dolphins *J. Exp. Biol.* **119** 265–74

[39] Combes S A and Daniel T L 2001 Shape, flapping and flexion: wing and fin design for forward flight *J. Exp. Biol.* **204** 2073–85

[40] Henderson D M 2003 The eyes have it: the sizes, shapes, and orientations of theropod orbits as indicators of skull strength and bite force *J. Vertebr. Paleontol.* **22** 766–78

[41] Coleman H W and Steele W G 2018 *Experimentation, Validation, and Uncertainty Analysis for Engineers* vol 8 (New York: Wiley)

[42] Araújo R, Polcyn M J, Schulp A S, Mateus O, Jacobs L L, Gonçalves A O and Morais M L 2015 A new elasmosaurid from the early Maastrichtian of Angola and the implications of girdle morphology on swimming style in plesiosaurs *Neth. J. Geosci.* **94** 109–20

[43] Massare J A 1988 Swimming capabilities of Mesozoic marine reptiles: implications for method of predation *Paleobiology* **14** 187–205

[44] O'Keefe F R 2002 The evolution of plesiosaur and pliosaur morphotypes in the Plesiosauria (Reptilia: Sauropterygia) *Paleobiology* **28** 101–12

[45] Benson R B J, Ketchum H F, Naish D and Turner L E 2013 A new leptocleidid (Sauropterygia, Plesiosauria) from the vectis formation (early barremian-early aptian; early cretaceous) of the isle of wight and the evolution of leptocleididae, a controversial clade *J. Syst. Palaeontol.* **11** 233–50